Inorganic Chemistry

Article

pubs.acs.org/IC

Brønsted Instead of Lewis Acidity in Functionalized MIL-101Cr MOFs for Efficient Heterogeneous (nano-MOF) Catalysis in the Condensation Reaction of Aldehydes with Alcohols

Annika Herbst, Anupam Khutia, and Christoph Janiak*

Institut für Anorganische Chemie und Strukturchemie, Heinrich-Heine-Universität Düsseldorf, Universitätsstrasse 1, D-40225 Düsseldorf, Germany

Supporting Information

ABSTRACT: Porous chromium(III) 2-nitro-, 2-amino-, and nonfunctionalized terephthalate (MIL-101Cr) metal organic frameworks are heterogeneous catalysts for diacetal formation from benzaldehyde and methanol (B−M reaction) as well as other aldehydes and alcohols. MIL-101Cr-NO_2 obtained by direct reaction between CrO_3 and 2-nitro-terephthalate showed the highest activity with 99% conversion in the B−M reaction in 90 min and turnover numbers of 114. The activity decreased in the order MIL-101Cr-NO_2 > MIL-101Cr > MIL-101Cr-NH_2. Within different samples of nonfunctionalized MIL-101Cr the activity increased with surface area. Methanol gas sorption of the different MIL materials correlates with the BET surface area and pore volume but not with the diacetalization activity. Benzaldehyde adsorption from heptane showed no significant difference for the different MILs. Gas sorption studies of CD_3CN to probe for a higher Lewis acidity in MIL-101Cr-NO_2 remained inconclusive. A high B−M catalytic activity of wet MIL-101Cr-NO_2 excluded significant contributions from coordinatively unsaturated Lewis-acid sites. pH measurements of methanol dispersions of the MIL materials gave the most acidic pH (as low as 1.9) for MIL-101Cr-NO_2, which significantly increased over MIL-101Cr (3.0) to MIL-101Cr-NH_2 (3.3). The increase in acidity is of short range or a surface effect to the heterogeneous MIL particles as protons dissociating from the polarized aqua ligands (Cr−OH_2) have to stay near the insoluble counteranionic framework. The variation in Brønsted acidity of MIL-101Cr-NO_2 > MIL-101Cr ≈ MIL-101Cr-NH_2 correlates with the withdrawing effect of NO_2 and the diacetalization activity. The catalytic B−M activity of soluble, substitution-inert, and acidic $Cr(NO_3)_3 \cdot 9H_2O$ supports the Brønsted-acid effect of the MIL materials. Filtration and centrifugation experiments with MIL-101Cr-NO_2 revealed that about 2/3 of the catalytic activity comes from nano-MOF particles with a diameter below 200 nm. The MIL-101Cr-NO_2 catalysts can be recycled five times with very little loss in activity. The diacetalization activity of MIL-101Cr-NO_2 decreases with the alcohol chain length from methanol over ethanol, *n*-propanol, *n*-butanol, to almost inactive *n*-pentanol, while conversions for benzaldehyde, paratolylaldehyde, 4-chlorobenzaldehyde, and cyclohexanone all reach 90% or more after 90 min.

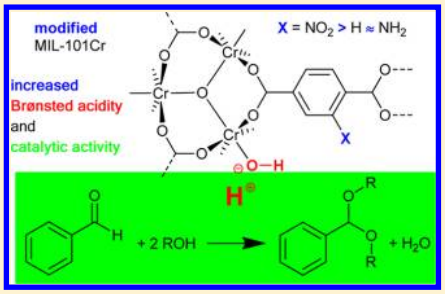

INTRODUCTION

In recent years metal organic frameworks (MOFs), also known as porous coordination polymers (PCPs), have gained enormous attention due to promising applications such as gas storage,[1] gas and liquid separation processes,[2] sensing,[3] drug delivery,[4] luminescence,[5] magnetism,[6] heterogeneous catalysis,[7] heat transformation processes,[8] and hosts for metal nanoparticles.[9] MOFs are composed of metal ions or clusters, connected through organic linkers which lead to versatile topologies and architectures. MOFs surpass classical porous materials such as zeolite or activated carbon in their permanent porosities, high surface areas, tunable pore sizes, and topologies.[10] In MOFs BET surfaces range typically between 1000 and 4000 m^2/g and pore apertures or channel diameters from 0.3 to 3.4 nm with pore volumes of up to 1.5 or 2 cm^3/g.

Currently, MOFs are investigated as heterogeneous catalysts for various organic reactions.[11] An advantage of MOFs over other related porous materials toward catalysis should be their high order and uniformity of the porous network for size- and shape-selective catalysis.[12] There is a current focus on the Lewis acidity/basicity in MOFs. Catalytic reactions of MOFs include Lewis-acid catalysis, Lewis-base catalysis, enantioselective catalysis, etc. MOFs having coordinatively unsaturated metal centers can potentially interact with the substrate and act as Lewis-acid catalyst.[11d,13,14] The role and increase of active metal sites for catalysis with MOFs was studied and critically discussed by DeVos and co-workers.[15,16] The presence of suitable functional groups either in the organic linkers or attached to the metal center can also influence the Lewis acidity and catalytic activity of MOFs.[17−21]

MIL-101Cr is a three-dimensional chromium−terephthalate-based porous material with the empirical formula $[Cr_3(O)(BDC)_3(F,OH)(H_2O)_2]$ (where BDC = benzene-1,4-dicarboxylate).[22] Its structure resembles the augmented MTN zeolite topology with pore diameters of about 2.9 and 3.4 nm (Figure

Received: March 22, 2014
Published: July 9, 2014

dx.doi.org/10.1021/ic5006456 | Inorg. Chem. 2014, 53, 7319−7333

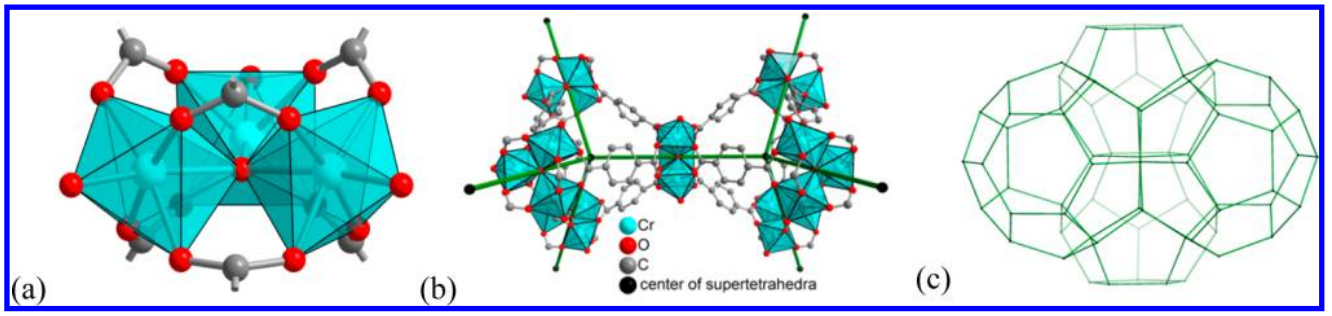

Figure 1. MIL-101Cr network with the (a) trinuclear $\{Cr_3(\mu_3\text{-}O)(O_2C-)_6(F,OH)(H_2O)_2\}$ building unit which forms the vertices of supertetrahedra (b). Vertex-sharing supertetrahedra (b) then form two types of mesoporous cages with pentagonal and hexagonal windows (c). For presentation of the pore and window size see Figure S1, Supporting Information.

1). MIL-101Cr has two terminal water molecules connected to the trinuclear $\{Cr_3(\mu_3\text{-}O)(O_2C-)_6(F,OH)(H_2O)_2\}$ building units with their octahedral Cr(III) ions (Figure 1a), which can be removed under high vacuum, thus creating Lewis-acid sites.[17,23] MIL-101Cr[8a] or its derivatives[8i] show remarkable stability toward water, which make them suitable for catalytic reactions involving water.

The catalytic activity of MIL-101Cr or its derivatives has been reported in the literature for various organic reactions such as oxidation of aryl sulfides to sulfoxides,[24] epoxidation of alkenes with H_2O_2,[25] or cyanosilylation of aldehydes.[26] Amine-grafted MIL-101Cr has proven to be a useful catalyst for Knoevenagel condensation reaction with high yield and high selectivity.[23,27] Pd loaded on amine-grafted MIL-101Cr has been used as catalyst for Heck reaction.[23] Similarly, Cu nanoparticles embedded in MIL-101Cr act as a high-performance catalyst for reduction of aromatic nitro compounds.[28] Recently, MIL-101Cr and its phospho-tungstic acid (PTA) composite material have been proven as efficient catalysts for aldehyde–alcohol reactions, including the benzaldehyde dimethyl acetal formation (cf. Scheme 1), albeit of low activity for MIL-101Cr only (24 h for 80% conversion).[29]

Scheme 1. Diacetalization of Benzaldehyde with Different Alcohols[a]

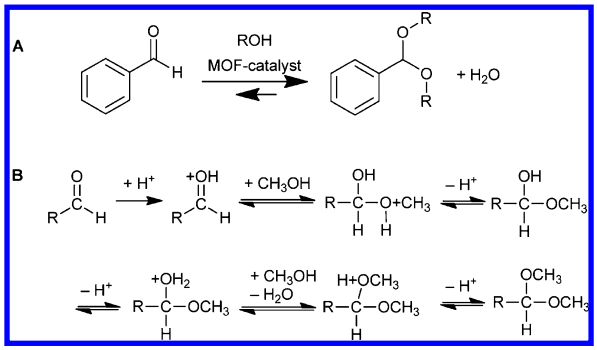

[a]R = Me, Et, ^{n}Pr, ^{n}Bu, $^nC_5H_{11}$, $PhCH_2$ and the Brønsted-acid (proton) catalyzed acetalization mechanism.[30,31].

Acetalization is an important technique to protect aldehyde or ketone groups in organic transformation reactions (Scheme 1). In homogeneous phase the reaction between the carbonyl substrate and the alcohol or trialkyl orthoformates as reagents is normally carried out in the presence of Brønsted acids (Scheme 1)[30,31] or Lewis-acidic transition-metal catalysts (Scheme 2).[32] The water formed in the equilibrium reaction has to be removed for quantitative conversion, which is typically done either azeotropically in a Dean–Stark apparatus or using trialkyl orthoformate as a water scavenger. The Lewis-acid catalysis mechanism is proposed as a simultaneous activation of the alcohol and the aldehyde by coordination at two available cis coordination sites (Scheme 2). Alcohol or alkoxide addition to the carbonyl group is then an intramolecular concerted reaction leading to a complexed hemiacetal or hemiacetalide (Scheme 2A or 2B, respectively). The reaction can proceed either through formation of an oxocarbenium ion, which subsequently undergoes external addition of ROH (Scheme 2A),[33] or by nucleophilic attack of ROH on the chelating hemiacetalide (Scheme 2B).[34] The intermediate metal hydroxide is then transformed to the metal aqua species by the protonated alcohol, and subsequently, the aqua ligand is substituted by the aldehyde.[34]

Irrespective of the mechanistic details, transition metals seem to be catalytically active when (a) two "active sites" in cis positions can easily be generated, e.g., by the presence of weakly coordinated ligands, and (b) the bonds between the metal center and the O donors are labile.[32–34] Also, a high charge of the metal ion is advantageous as it facilitates polarization of the metal–carbonyl substrate bond and promotes deprotonation of the coordinated ROH reagent. Both effects favor nucleophilic attack onto the coordinated C=O group.[32] For chromium(III) and MIL-101Cr the application of these principles creates a dilemma: If two cis positions are needed the Cr ions in MIL-101Cr will not have two "active sites" in cis position unless one assumes missing dicarboxylate linkers. Such missing linkers in MOFs can be possible as recently demonstrated for UiO-66.[20,35] For the moment we are not aware of similar studies on linker deficiencies in MIL-101Cr as for UiO-66. However, from coordination chemistry principles it can be envisioned that construction faults during the metal–ligand assembly in inert Cr(III) MOFs cannot easily be corrected as in labile Zn(II) MOFs with a pronounced dissociation equilibrium. Thus, there will be a certain degree of imperfections, such as missing linkers also in Cr(III) MOFs. However, one could also imagine that only the carbonyl compound is activated on one Lewis-acid site while the alcohol stays in the outer coordination sphere. Even then, Cr(III) does not form labile but inert complexes. Even if there is initially a vacant Lewis-acidic site on chromium the released water from the condensation reaction will occupy the unsaturated metal sites. Then, the rate constant for the water exchange in $[Cr(H_2O)_6]^{3+}$ is a very small 2.4×10^{-6} s^{-1} (at 298.15 K).[36] A recent comprehensive review on transition-metal complexes in the synthesis of acetals does not list chromium as a catalyst.

dx.doi.org/10.1021/ic5006456 | Inorg. Chem. 2014, 53, 7319–7333

Scheme 2. Proposed Mechanisms for Transition-Metal-Catalyzed Acetal Formation[a]

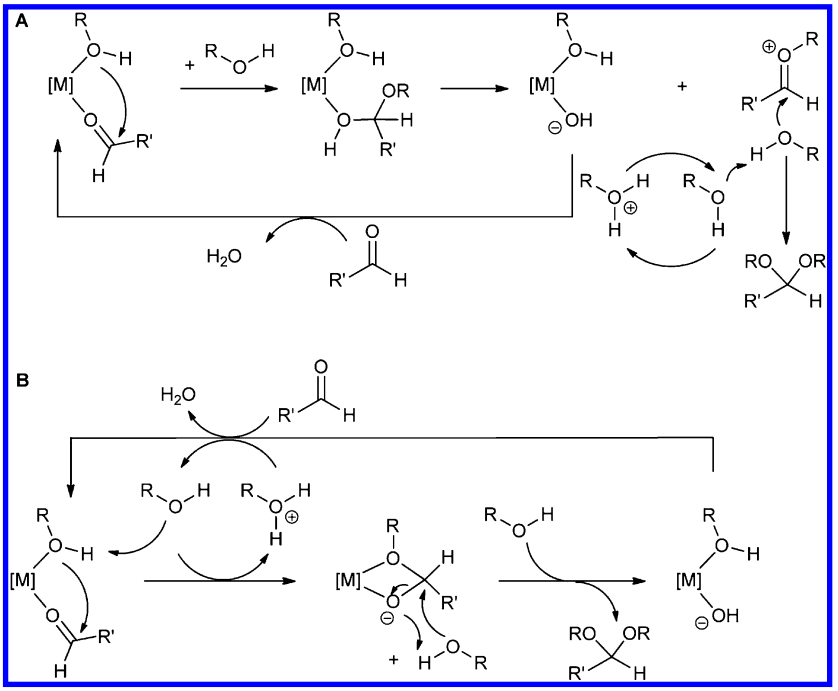

[a]Adapted from refs 32−34.

Table 1. Porosity and Particle Size Properties of MIL-101-Cr Materials

	BET surface area (m^2/g)[a]		total pore volume (cm^3/g)[b]			
materials	before	after catalysis[e]	before	after catalysis[e]	methanol loading (g/g)[c]	particle diameter ± standard deviation (σ) (nm)[d]
1a	3055	3100[e]	1.51	1.56	1.08	479 ± 150
1b	2763	2712	1.45	1.43	n.d.	330 ± 160
1c	2509	2749	1.15	1.42	n.d.	300 ± 70
2-NO_2-d	2429	2377, 2421[f]	1.32	1.35, 1.44[f]	0.89	380 ± 100
2-NO_2-ps	1353	1550	0.74	0.89	n.d.	280 ± 50
3-NH_2-ps	2920	2711[g]	1.60	1.53[g]	1.08	220 ± 30

[a]Calculated in the pressure range $0.05 < p/p_0 < 0.2$ from N_2 sorption isotherm at 77 K. BET error margin is 20−50 m^2/g. [b]Calculated from N_2 sorption isotherm at 77 K ($p/p_0 = 0.95$) for pores ≤ 20 nm. [c]Gravimetric methanol uptake capacity calculated from methanol sorption isotherm at 298 K (see also Figure 4 below) at $p/p_0 = 0.8$ (condensation effects possible at higher levels); n.d. = not determined. [d]Obtained by dynamic light scattering (DLS) of a particle suspension in methanol (see Figures S10−S12, Supporting Information). [e]After 90 min catalysis unless stated otherwise. See corresponding N_2 sorption isotherms as Figure S3, Supporting Information. [f]After five catalytic runs with 90 min each. [g]After a catalytic run for 24 h.

Rather, chromium is in a list of precursors noted as less or completely ineffective (see conclusions in ref 32).

Many solid materials such as zeolite,[37] silica gel,[38] and aluminosilicate[39] have been used as heterogeneous catalysts for the acetalization reaction of aldehydes with trimethyl orthoformate. Methanol has been reported for the condensation with aldehyde under refluxing condition, catalyzed by siliceous mesoporous material MCM-41.[40] Use of methanol in this condensation reaction would be advantageous because of its availability. Recently, MOF-catalyzed acetalization of aldehydes with methanol has been reported with $Cu_3(BTC)_2$[41] or MIL-101Cr/PTA composite materials.[29] In the present work, we study the effect of nitro and amino groups in MIL-101Cr (**1**) with its (postsynthetic) derivatives MIL-101Cr-NO_2 (**2-NO_2**) and MIL-101Cr-NH_2 (**3-NH_2-ps**) as heterogeneous catalysts for the condensation reaction of aldehydes with different alcohols (Scheme 1). Thereby, we also consider the effect of nano-MOFs in the catalytic activities of **2-NO_2-d**. The different porosity, particle size, and sorption properties **1**−**3** should contribute to a better understanding of how postsynthetic modifications influence the catalytic behavior of MOFs. We verify the Brønsted acidity of chromium MIL-101 which originates from aqua ligands versus the role of Lewis acidity of possible open metal sites. Lewis acidity has been the recent focus on the modification and tuning of MILs for catalytic applications[20,21,42] but does not seem to have taken into account the simultaneous Brønsted acidity of these MOFs.[43,44]

RESULTS AND DISCUSSION

Synthesis and Porosity. Three different batches of MIL-101Cr samples (**1a**−**c**) with different surface areas and pore volumes were reproducibly obtained by modifications in the synthesis route (Table 1). Sample **1a** was synthesized hydrothermally through a base-mediated reaction of $Cr(NO_3)_3$ and terephthalic acid.[45] MIL **1b** and **1c** were prepared through reaction of $Cr(NO_3)_3$ and terephthalic acid under acidic hydrothermal conditions[22] but differ in the washing part of

dx.doi.org/10.1021/ic5006456 | Inorg. Chem. 2014, 53, 7319−7333

their activation procedure (see below). The different batches of **1a−c** were each obtained reproducibly 2−3 times.

From the reaction of CrO_3 with 2-nitroterephthalic acid, MIL-101Cr-NO_2 (**2-NO_2-d**) was synthesized directly under hydrothermal conditions as reported in the literature.[8b] In addition, the postsynthetic modification of MIL-101Cr yielded also MIL-101Cr-NO_2 (**2-NO_2-ps**) and MIL-101Cr-NH_2 (**3-NH_2-ps**).[46,47] The suffix "-d" denotes direct synthesis, and "-ps" denotes postsynthetic synthesis. Organic linkers bearing functional groups may be incompatible for reaction under hydrothermal condition. Postsynthetic modification (PSM) is an alternative technique to introduce suitable functional groups in the material.[48] Here, we used nitration of MIL-101Cr with mixed acid (conc. HNO_3/conc. H_2SO_4) to yield **2-NO_2-ps**. MIL-101Cr-NH_2 (**3-NH_2-ps**) was then prepared through subsequent reduction of **2-NO_2-ps** with $SnCl_2$ and conc. HCl (Scheme 3).

Scheme 3. Schematic Representation of the Synthesis of MIL-101Cr-NO_2 (2-NO_2-ps, 2-NO_2-d) and MIL-101Cr-NH_2 (3-NH_2-ps) through Postsynthetic (-ps) Modification of MIL-101Cr or by Direct (-d) Synthesis

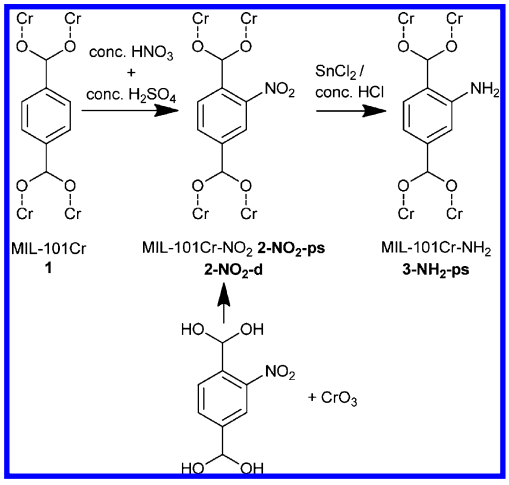

Analyses and catalytic studies were carried out on samples which were purified (activated) as follows: Compounds **1a−c** were purified by washing with H_2O, DMF, and ethanol, followed by 12 h stirring in DMF at room temperature and 6 h at 110 °C, concluded by 12 h stirring in ethanol at room temperature and 3−5 h at 90 °C with a final washing with water. Compound **1c** was additionally treated with boiling water for 12 h. The amount of solvent was 90 mL per washing cycle (see Supporting Information for details). Compounds **2-NO_2-d** and **-ps** as well as **3-NH_2-ps** were activated by washing three times with water (see Supporting Information for details). Finally, the materials **1−3** were collected by centrifugation and dried at 70 °C overnight. For use in catalysis the materials **1−3** were dried in vacuum (10^{-6} Torr) for 48 h at 30 °C and stored under nitrogen unless stated otherwise. Activation of MOF materials is particularly important to obtain materials with high surface area and pore volume. Different synthesized batches of MOF samples may have different surface area. Many parameters such as crystal defects and phase purity or the presence of guest molecules may influence the surface area of the materials. Previous studies[17] showed the presence of a significant amount of unreacted terephthalic acid within the pores of MIL-101Cr, which is very difficult to remove from the pores, leading to a decrease in surface area.

All compounds were characterized by powder X-ray diffractometry (PXRD) and surface area analysis. PXRD patterns match well with the simulated MIL-101Cr patterns (Figure 2a), which suggest retention of framework structures after postsynthetic modification. N_2 sorption isotherms showed typical type I isotherms, characteristic of a microporous material (Figure S2, Supporting Information). BET surface areas were calculated from N_2 sorption isotherms at 77 K. MIL-101Cr (**1a**) from base-mediated synthesis has a significantly higher BET surface area and pore volume than the acid-synthesized materials **1b** and **1c** (Table 1). The higher surface area of **1a** can be ascribed to the better solubility of terephthalic acid in alkaline aqueous solution. Purification of **1b** and **1c** differs by an additional final overnight washing cycle in hot water for **1c** (see Supporting Information for details).

Thermogravimetric analyses of **1−3** (dried at 10^{-6} Torr for 48 h at 30 °C) in Figure 2b showed that up to 200 °C a weight loss of less than 8% occurred.

Catalytic B−M Reaction. Conversion of benzaldehyde with methanol to benzaldehyde dimethyl acetal (B−M reaction) in the presence of different catalysts (Scheme 1) was screened, and conversion was followed by gas chromatography. The alcohol was added in excess with the ratio between alcohol to benzaldehyde as 50:1. For all experiments 10 mg of the catalyst was used, which corresponds to a molar ratio of chromium to benzaldehyde of 1:80. The materials **1−3** were tested under identical conditions.

For the three nonfunctionalized MIL-101Cr materials **1a−c** it can be stated that a higher surface area leads to higher conversion of benzaldehyde to dimethylacetal (Figure 3, Table 2). After 90 min, the highest surface area sample **1a** (S_{BET} = 3055 m^2/g) shows a conversion of 73%. A notably higher activity could be observed for the functionalized samples **2-NO_2-d** and **3-NH_2-ps** (Figure 3, Table 2). After only 20 min a conversion of 83% and after 90 min a quantitative conversion of 99% was measured for **2-NO_2-d**. The higher activity of **2-NO_2-d** indicates a positive effect on the catalytic activity by the NO_2 group because the surface area of 2429 m^2/g of **2-NO_2-d** is 20% lower than the surface area of **1a** (3055 m^2/g). The material **2-NO_2-ps** with the lowest surface area of 1352 m^2/g among all samples **1−3** shows a lower catalytic activity than **1a** (73%), but with 56% conversion after 90 min its activity is still higher than for the lower surface materials **1b** (35%) and **1c** (19%). In the UiO-66Zr-catalyzed cyclization of (+)-citronellal to isopulegol and its isomers and - conversion of geraniol in the Oppenhauer oxidation with furfural the activity of UiO-66Zr-NO_2 was also strongly increased over the nonfunctionalized parent compound.[21] Also, the Meerwein reduction of 4-*tert*-butylcyclohexanone with isopropanol proceeded much faster with UiO-66Zr-NO_2.[20] Molecular modeling studies suggested that the nitro group lowers the adsorption and activation free energy of the reaction.[21]

Compound **3-NH_2-ps**, which is functionalized with NH_2 groups, shows a slightly higher catalytic activity (77%) than the nonfunctionalized MILs **1a** (73%) but lower than **2-NO_2-d** (99%), although **3-NH_2-ps** has a higher surface area than **2-NO_2-d** (cf. Table 1). This finding contrasts with the observed lowest activity for UiO-66Zr-NH_2 in the UiO-66Zr-X-catalyzed cyclization of (+)-citronellal to isopulegol and its isomers. There, the activity of UiO-66Zr-NH_2 was slightly lower than that of the parent compound UiO-66Zr.[21] In the UiO-66-Zr-

dx.doi.org/10.1021/ic5006456 | Inorg. Chem. 2014, 53, 7319−7333

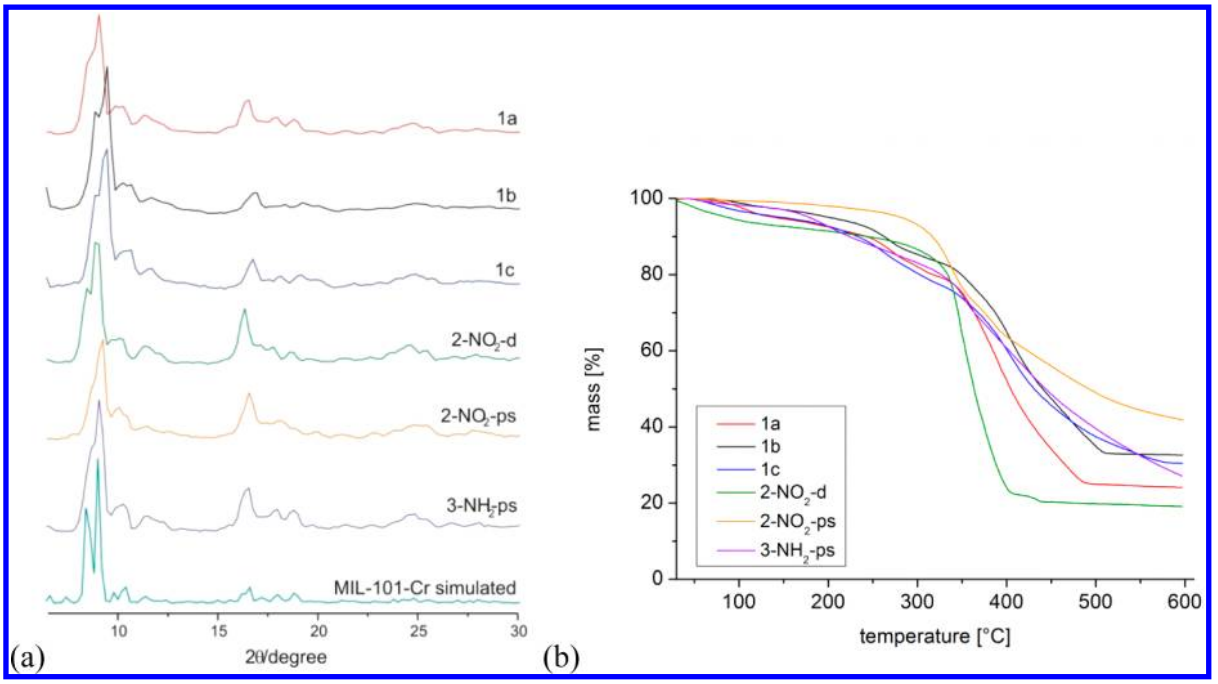

Figure 2. (a) PXRD patterns of MIL-101Cr samples. (b) Thermogravimetric analysis of **1**−**3**.

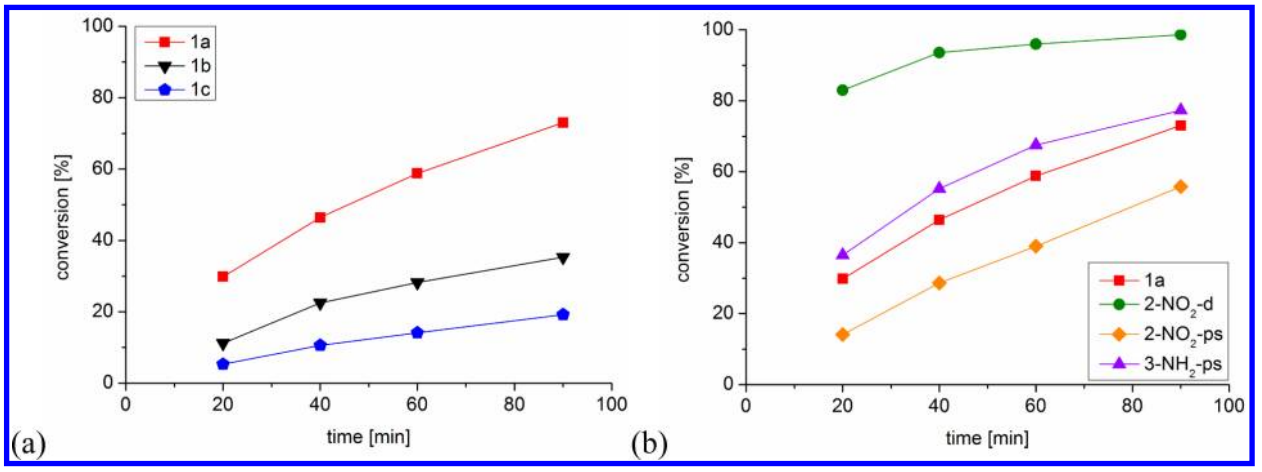

Figure 3. Time-dependent conversion of benzaldehyde to dimethyl acetal over 90 min: (a) Nonfunctionalized MIL **1a**−**c** and (b) **1a** and functionalized MIL-101 derivatives **2-NO$_2$-d**, **2-NO$_2$-ps**, and **3-NH$_2$-ps** (right).

Table 2. Catalytic Activities in the Acetalization of Benzaldehyde with Methanol with Different MIL-101Cr Catalysts[a]

materials	conversion [%]	TON[b]	TOF [h^{-1}][c]
1a	73	84	56
1b	35	40	27
1c	19	22	15
2-NO2-d	99	114	76
2-NO2-d-wet	74	85	57
2-NO2 ps	56	65	43
3-NH2 ps	77	89	59

[a]Standard reaction conditions: reaction time 90 min, benzaldehyde (340 μL, 3.34 mmol), methanol (6.7 mL, 166 mmol), total volume 7.04 mL, catalyst (10 mg =2.9 × 10^{-2} mmol chromium (2/3 of total n(Cr) = 0.043 mmol)). Every reaction was performed at least in duplicate to ascertain reproducibility. [b]TON = mol of product/mol of chromium. [c]TOF = mol of product/(mol of chromium·time(h))

catalyzed cyclization of citronellal the activity as log k_x shows a strong correlation with Hammett's σ values for the linker.[21]

The BET surface areas of **1**−**3** were determined again after the catalytic runs and found to be largely unchanged within experimental error (**1a**, **1b**, **2-NO$_2$-d**) or even slightly increased (**1c**, **2-NO$_2$-ps**), and only for **3-NH$_2$-ps** there was a slight decrease (Table 1). The increase of the surface area can be assigned to the soaking and washing of the MIL material with methanol during and after the catalysis run before drying for the sorption measurement. Clearly, the materials **1**−**3** retain their porosity (Table 1). Also, the phase identity and crystallinity **1**−**3** was unchanged after the catalytic runs as evidenced by powder X-ray diffraction (compare Figure 2 and Figures S4 and S15, Supporting Information).

For material **3-NH$_2$-ps** the NH$_2$ groups on the terephthalate ligand could react with benzaldehyde in a Schiff base reaction. This possibility was, however, not supported by IR spectroscopy (Figure S6, Supporting Information). In the IR spectrum

dx.doi.org/10.1021/ic5006456 | Inorg. Chem. 2014, 53, 7319−7333

of **3-NH_2-ps** no additional signal for a N=C bond could be detected after the catalytic run (which would have been expected as a very strong band between 1600 and 1630 cm^{-1}). The XRD stayed unchanged and confirmed that material **3-NH_2-ps** was still intact and crystalline after catalysis (Figure S6, Supporting Information) and the surface area decreased only slightly (Table 1).

Methanol and Benzaldehyde Adsorption. From all catalysts **2-NO_2-d** shows by far the best performance with near quantitative conversion in less than 90 min, so that we studied its properties in more detail in comparison to the other materials. If the catalytic reaction takes place inside the pores then the kinetics and thermodynamics of the substrate adsorption and product desorption may also determine the conversion rate. In order to rule out or support this effect, methanol gas ad- and desorption isotherms (Figure 4), which

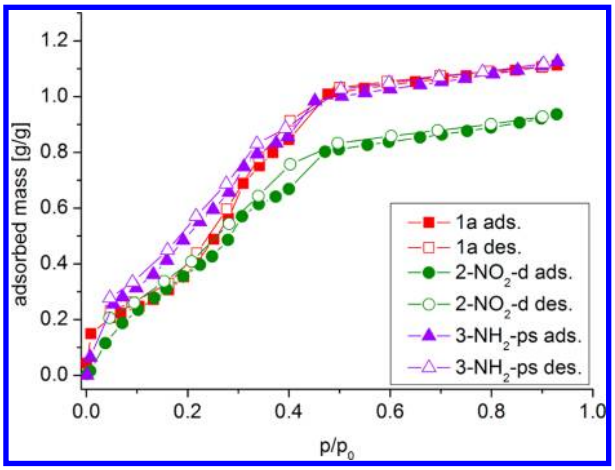

Figure 4. MeOH gas sorption isotherms (closed symbols for adsorption, and open symbols for desorption).

reflect the thermodynamic sorption behavior, were collected for **1a**, **2-NO_2-d**, and **3-NH_2-ps** on a Quantachrome iQ MP with all gas option (see Supporting Information for experimental details). The maximum MeOH uptake correlates with the BET surface area and pore volume (Table 1). There are slight differences in the onset of MeOH uptake (Figure 4). MIL **1a** and **3-NH_2-ps** reach the uptake of 0.15 g MeOH/g MIL already at $p/p_0 < 0.05$, while MIL **2-NO_2-d** shows this uptake not until $p/p_0 > 0.05$. Still, the differences in the MeOH gas uptake are not significant enough and do not follow the activity order **2-NO_2-d** > **3-NH_2-ps** > **1a**.

Considering that MeOH is present in 50-fold excess compared to benzaldehyde, the uptake of benzaldehyde may have a more significant effect on the activity. In the acetaldehyde–phenol condensation with MIL-101/PTA the acetaldehyde uptake capacity PTA > MIL-101/PTA > MIL-101 correlated with the activity.[29] Therefore, the time-dependent liquid-phase adsorption of benzaldehyde from a heptane solution was measured with gas chromatography (Figure 5).

The different MILs show an uptake of benzaldehyde between 0.45 (**2-NO_2-d**) and 0.71 g/g (**1a**). The benzaldehyde adsorption occurs within the first 5 min and does not change anymore over the next 15 min. The slight fluctuation over time in Figure 5 indicates the experimental error, so that small differences, e.g., between the 5 and 10 mg samples, should not be overinterpreted. The uptake in the general order **1a** > **3-NH_2-ps** > **2-NO_2-d** follows the trend in surface area (cf. Table 1).

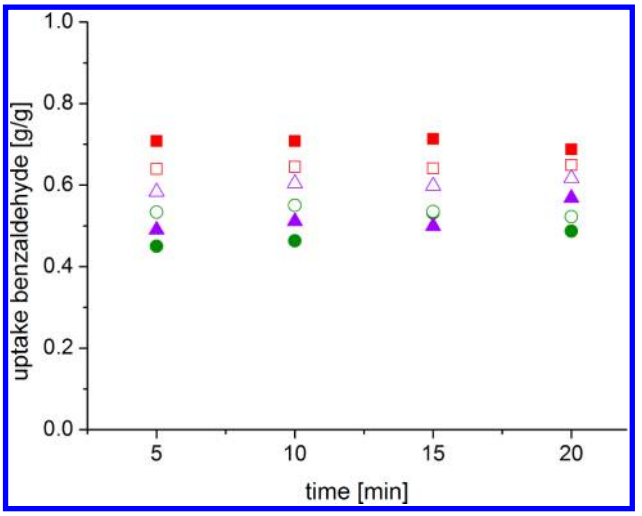

Figure 5. Benzaldehyde adsorption from heptane solution: (red squares) **1a**, (green circles) **2-NO_2-d**, and (purple triangles) **3-NH_2-ps**; filled symbols belong to 5 mg of MIL and the empty symbols to 10 mg of MIL sample. Uptake was calculated from the gas chromatogram peak area (initial benzaldehyde amount − benzaldehyde left after equilibration) per mass of MIL. *n*-Dodecane was used as internal standard. The molar ratio of benzaldehyde to Cr was 10:1 for 5 mg of MIL and 5:1 for 10 mg of MIL sample (see Supporting Information for experimental details).

Thus, the methanol and benzaldehyde adsorption studies do not provide evidence that the substrate adsorption has a decisive influence on the catalytic activity. In consequence, the high catalytic activity of **2-NO_2-d** compared to **1a** and **3-NH_2-ps** should be reasoned by electronic effects from the nitro group.

Lewis Acidity and Brønsted Acidity. The nature of the active sites in MIL-101Cr is still an open question here: Lewis-acid vacant Cr(III) sites or Brønsted-acid sites from polarized acidic aqua ligands (Cr−OH_2), perhaps enhanced by the acid treatment of MIL-101Cr upon modification?[15] Metal ions polarize and thereby increase the acidity of their aqua ligands. For $[Cr(H_2O)_6]^{3+}$,[36,49] $[CrBr(en)(H_2O)_3]^{2+}$,[50] $[Cr(en)(NH_3)(H_2O)_3]^{3+}$,[51] and some other Cr(III) aqua–amine complexes[52] the first dissociation constant is estimated at $pK_a \approx 4$. The first acid dissociation constants for $[Cr(III)(NH_3)_n(OH_2)_{6-n}]^{3+}$ lies between 4.4 and 5.3 depending on the number of aqua ligands, their cis, trans, fac, or mer orientation.[53] The acidity constant of *cis*-$[Cr(C_2O_4)_2(NCS)(H_2O)]^{2-}$ has been determined spectrophotometrically to $pK_a = 7.06 \pm 0.18$.[54] It has been shown that both Lewis and Brønsted acidity and thereby the catalytic activity of MIL-100Fe can be further enhanced via creation of additional active sites using a postsynthesis acid treatment.[15,55]

For the materials **1**–**3** we have to decide here if the activity of the benzaldehyde acetalization depends on the Lewis or Brønsted acidity of the vacant Cr or aqua-ligand Cr−OH_2 sites, respectively. Before reaction each catalyst was activated under identical conditions (drying under high vacuum of 10^{-6} Torr for 48 h at 30 °C unless stated otherwise) and stored in a glovebox under anhydrous and anaerobic conditions. Thus, we can assume that the number of dehydrated and hydrated chromium sites is very similar in **1**–**3**. Therefore, we suggest, so far, that the Lewis or Brønsted acidity of the Cr(−OH_2) sites

dx.doi.org/10.1021/ic5006456 | Inorg. Chem. 2014, 53, 7319−7333

gets stronger with an electron-withdrawing $-NO_2$ group on the linker and close to the metal site (see below).[19]

Lewis Acidity. Chemisorption of CD_3CN has been used to measure the number and strength of the Lewis-acid sites.[20] The C≡N stretching frequency is increased by about 40 cm^{-1} for CD_3CN chemisorbed at a Lewis-acid chromium site (Cr-$NCCD_3$) compared to physisorbed CD_3CN. For **1a** and the nitro-modified material **2-NO_2-d**, chemisorption of CD_3CN was investigated by infrared spectroscopy following sample activation as for catalysis (drying under high vacuum of 10^{-6} Torr for 48 h at 30 °C) (Figure 6, see Supporting Information for more details).

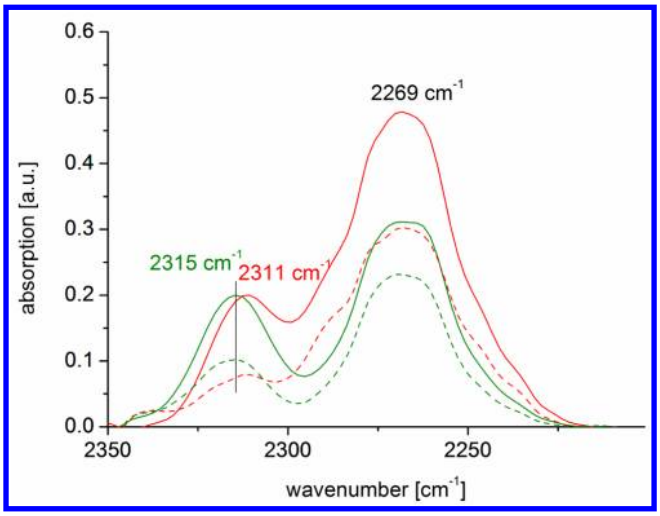

Figure 6. Time-dependent IR spectra for the CD_3CN chemisorption on **1a** (red) and **2-NO2-d** (green). Spectra start at 30 min after the beginning of CD_3CN exposure and are measured every 10 min up to 2 h: (dotted line) measured after 30 min, (solid line) measured after 2 h (bands at intermediate times are not shown for clarity).

Spectra show a time-dependent increase of adsorption both for physisorbed CD_3CN at 2269 cm^{-1} (overlaps with the band for free, gaseous CD_3CN) and for chemisorbed CD_3CN at 2311 and 2315 cm^{-1} for **1a** and **2-NO_2-d** respectively. For chemisorbed CD_3CN the CN stretching frequency was reported to be 2326−2321, 2304, 2305, and 2298 in MIL-100Al, Fe, Cr, and UiO-66, respectively.[20,44] The large hypsochromic frequency shift versus free CD_3CN for MIL-100Al is associated with the high Lewis-acid strength of Al^{3+}.[44] Assuming the same molar amount of Lewis-acid sites in **1a** and **2-NO_2-d**, normalization of the chemisorbed bands then shows a higher CD_3CN physisorption for **1a** due to its higher surface area (cf. Table 1). The slight hypsochromic shift of the signal of **2-NO_2-d** versus **1a** may signify stronger Lewis-acid properties for the nitro-modified material.[44] We note that coordination of CD_3CN like coordination of CO to the H atom of an aqua ligand[43] will also result in a hypsochromic shift with respect to free CD_3CN. Thus, the acetonitrile test showed the same amount (by absorption) and a very similar strength (by wavenumber) of Lewis-acid sites in **1a** and **2-NO_2-d**. Thereby, we conclude from the test that the catalytic difference cannot be explained by differences in Lewis acidity as these could not be verified.

Acetalization of aldehydes is a condensation reaction, generating water within each formula conversion. From adsorption studies of water on MOFs it is known that the metal centers are coordinated first by the water molecules.[8e] Thus, even if the catalyst exhibits coordinative unsaturated sites (CUS) at the beginning, in the course of the reaction they will be coordinated by the released water, thereby blocking initially active Lewis-acid sites.[43] Hence, for the most active catalyst **2-NO_2-d** the effect of wetting (wetness effect) was tested. For this experiment 10 mg of vacuum-dried **2-NO_2-d** was suspended in H_2O (5 mL) and stirred for 20 min at room temperature. The solid was separated by centrifugation, and the supernatant solution was removed. The powder was dried in air at room temperature for 48 h. After this drying period the material **2-NO_2-d-wet** still contained about 48 wt % water, determined by thermogravimetry (see Figure S16, Supporting Information), and was employed as a catalyst under otherwise identical reaction conditions (Figure 7).

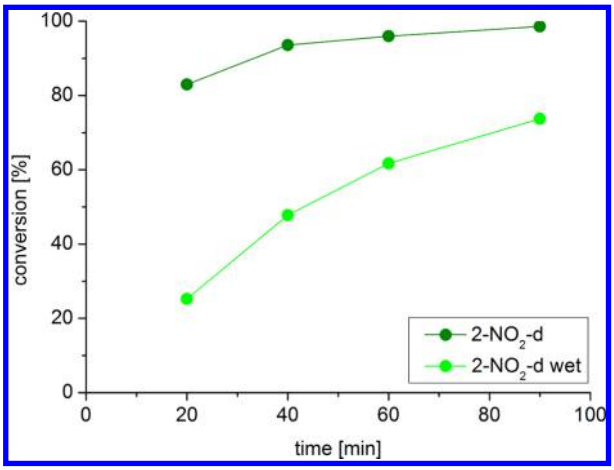

Figure 7. Activity of **2-NO_2-d** after an additional wetting with water.

After wetting, **2-NO_2-d-wet** shows reduced catalytic activity, especially at the beginning of the reaction, but reaches 74% conversion after 90 min, which still puts **2-NO_2-d-wet** among the high active materials (cf. Table 2). The loss in activity can be ascribed to the initial pore filling with water and, in part, to the adverse effect of water in the equilibrium formation of the product.[56] However, from the still high activity of this water-filled MOF it becomes quite clear that vacant Lewis-acid chromium sites are not needed for catalytic activity.

When the B−M reaction was carried out with the corresponding amount of chromium(III) nitrate nonahydrate as a catalyst under otherwise identical but homogeneous conditions even faster reaction rates and higher conversions were observed (see also Figure 13 below and Figure S9, Supporting Information). Hexaaquachromium(III) is very inert to ligand substitution with a rate constant for the water exchange in $[Cr(H_2O)_6]^{3+}$ of 2.4×10^{-6} s^{-1} (at 298.15 K).[36]

These last two observations lend strong support to the already indicated Brønsted-acid catalysis from deprotonation of the aqua ligands (see above) rather than Lewis-acid catalysis.

The high activity of $Cr(NO_3)_3 \cdot 9H_2O$ also excludes that the higher activity of dry versus wet **2-NO_2-d** (cf. Figure 7) is due to the known water uptake capacity of about 1 g H_2O/g MIL-101.[8i] The hydrated Cr(III) salt with the hexaaquachromium-(III) cation lacks a significant water binding capacity.

Brønsted Acidity and pH. A Brønsted acid should be verifiable by its pH change to a solvent. Consequently, the pH value of catalysts **1a**, **2-NO_2-d**, and **3-NH_2-ps** were measured in methanol. The pH was assessed using two different procedures.

dx.doi.org/10.1021/ic5006456 | Inorg. Chem. 2014, 53, 7319−7333

First, the pH was measured in slowly stirred suspensions of the dried MIL-101 powders in methanol. For the second procedure methanol was dropped onto MIL-coated KBr disks, and the pH of the wetted MIL surface was measured with a flat membrane electrode. Both methods show the same trend of pH value, that is, the pH is highest for **3-NH_2-ps** intermediate for **1a** and lowest for **2-NO_2-d** (Table 3). A higher concentration of MIL probes (10 mg of MIL in 6.7 mL of methanol versus 1 mg of MIL in 4 mL of methanol) approached the pH of the surface measurement of the MIL-coated KBr disk. Noteworthy, the pH values were only lowered in the near vicinity of the MIL particles. This explains the lower pH of the more concentrated suspension and of the wetted MIL-KBr coating. The pH values immediately rose for the supernatant MeOH solvent upon sedimentation of the particles when stirring was stopped. The suspensions were also filtered through a syringe filter and afterward centrifuged at 22 000 rpm for 40 min. By DLS it could be shown that the MIL material was completely removed. For the filtrates a much higher pH value was measured than with MIL sample, which shows clearly that the acidity originates from the MIL framework. Protons dissociating from the aqua ligands (Cr−OH_2) will leave a negatively charged hydroxyl group (Cr−OH^-). Thus, the insoluble framework will be the counteranion of the proton. By the electroneutrality principle the proton has to stay near the anionic framework. Hence, the Brønsted acidity of the MIL-101 compounds is a surface effect. At least in methanol it was verified that the acidity did not leach much into the surrounding liquid (see Supporting Information for pH measurements of the MIL materials in water). In methanol the variation in Brønsted acidity of **3-NH_2-ps** <**1a** < **2-NO_2-d** follows the electron-donating effect of NH_2 and the electron-withdrawing effect of NO_2.

Table 3. pH Values of the MIL-101 Materials and $Cr(NO_3)_3$ $9H_2O$ in Methanol[a]

material	pH value: methanol suspension	pH value: KBr disk coated with material
methanol	7.6	
KBr, not coated		6.6
1a	3.9,[b] 5.9[c]	3.0
2-NO_2-d	2.6,[b] 5.3[c]	1.9
3-NH_2-ps	–,[b] 6.6[c]	3.3
filtrate from **1a**[d]	6.2	
filtrate from **2-NO_2-d**[d]	6.3	
$Cr(NO_3)_3$ $9H_2O$[e]	1.4	

[a]See Supporting Information for more details. [b]A 10 mg amount of MIL in 6.7 mL of MeOH. [c]A 1 mg amount of MIL in 4 mL of MeOH. [d]Fitrate of a suspension of 10 mg of MIL sample in 6.7 mL of MeOH (0.2 μm syringe filter, centrifuged at 22 000 rpm for 40 min). [e]A 12 mg amount in 6.7 mL of MeOH.

Also, chromium nitrate nonahydrate in methanol yields a very acidic solution (Table 3) such that its high catalytic activity (see below) is due to the large proton concentration of the solution.

Brønsted acidity arising from coordinated hydroxyl groups, belonging to the framework, or water molecules was investigated by infrared spectroscopic studies of interaction of CO with monomeric or multimeric water species in the case of MIL-100Al.[44] pH measurements of the MIL-101 probes support the assumption that the high activity of, especially, **2-NO_2-d** orginates from the Brønsted-acid nature of the catalysts.

Filtration Tests. The MIL materials in this study were introduced as heterogeneous catalysts. In order to prove that no leaching occurs, the materials were tested in filtration experiments. After approximately 50% conversion the catalyst was separated by centrifugation at 6000 rpm and subsequent filtration from the reaction mixture using a 0.2 μm (200 nm) syringe filter. The possible increase in conversion was continued to be monitored on the visually clear solution by GC. For the solution from MIL **2-NO_2-d** the reaction did indeed continue with only a slightly lower conversion rate than for the nonfiltered reaction (Figure 8a). In contrast, for **1a** and **1b** the catalytic reaction came to a stop after filtration of the solid MIL compound (**1c** was not tested due to the low conversion rate). Reaction with **2-NO_2-ps** showed only a slight increase of 7% conversion after filtration (Figure S8, Supporting Information). Additionally, the B−M acetalization reaction was performed without MIL catalysts but under otherwise identical conditions. No conversion was observed for the first 3 h. After 24 h reaction time 26% 1,1-dimethoxytoluene had formed

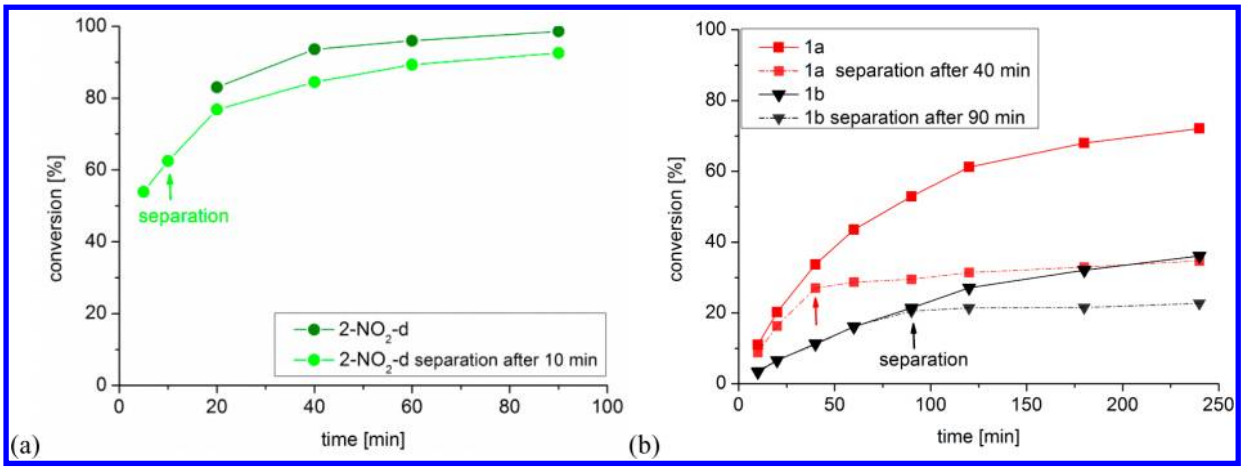

Figure 8. (a) Time conversion plot for **2-NO_2-d** and **2-NO_2-d** with attempted separation (6000 rpm centrifugation plus 0.2 μm filtration) of the catalyst completed after 5 min. (b) Time conversion plot for **1a** and **1b**; separation of **1a** completed after 40 min and of **1b** completed after 90 min (marked by arrows).

dx.doi.org/10.1021/ic5006456 | Inorg. Chem. 2014, 53, 7319−7333

(Figure S7, Supporting Information). This observation is consistent with previous studies.[29,41]

Two explanations are possible. On one hand, some leaching of Cr(III) species could have occurred. In a comparative test experiment with 4.2×10^{-5} mol of $Cr(NO_3)_3$, which corresponds to the amount of chromium(III) in 10 mg of MIL, a conversion of 94% was measured after 20 min (Figure S9, Supporting Information). As a consequence, soluble Cr(III) species have a high catalytic activity for acetalization of benzaldehyde. On the other hand, it is also comprehensible that some of the MIL particles are smaller than the 200 nm (0.2 μm) pore size of the syringe filter. Such nano-MOFs could form a clear colloidal solution and further act as catalyst system. DLS measurements have shown that the particle diameter distribution is quite broad (Table 1, Figure S10 and S11, Supporting Information). SEM pictures show that the particles of **2-NO_2-d** are smaller than **1a** (Figure 9).

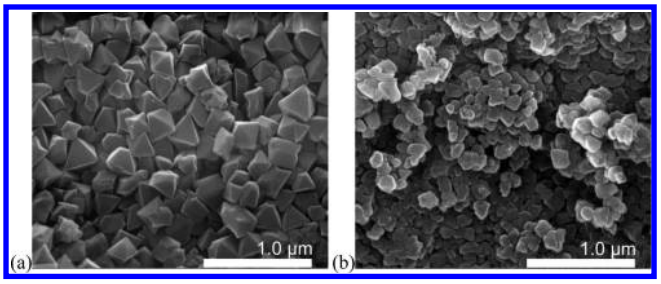

Figure 9. SEM pictures of (a) **1a** and (b) **2-NO_2-d**.

As a consequence, the filtrates of the reaction solutions were checked by DLS, TEM, and atomic absorption spectroscopy (AAS) for their particle and chromium content (Table 4, Figure 10). It is evident that the functionalized MILs **2-NO_2-d, -ps**, and **3-NH_2-ps** give rise to smaller particles which can pass through 200 nm filters.

Table 4. DLS and AAS Results of Filtrates

materials	time of filtration (min)[a]	DLS particle diameter ± standard deviation (σ) (nm) in filtrate[b]	AAS Cr(III) concentration (mg/L) in filtrate[c]
1a	90	n.d.	n.d.
1b	90	n.d.	n.d.
1c	90	n.d.	n.d.
2-NO_2-d	5	245 ± 117[c]	Cr detected, ~0.003
2-NO_2-d	90	131 ± 52[c]	0.04
2-NO_2-d	90 in 5th run	187 ± 66[c]	0.02
2-NO_2-ps	90	161 ± 57[c]	0.005
3-NH_2-ps	90	171 ± 54[c]	0.02

[a]From MeOH/benzaldehyde dispersion at 25 °C, filtered with a 0.2 μm (200 nm) syringe filter. [b]See Figure S13, Supporting Information. [c]n.d. = not detected; the detection limit for AAS is 0.003 mg/L.

By AAS, chromium could only be detected in the filtrates of **2-NO_2-d**, **2-NO_2-ps**, and **3-NH_2-ps** but not in **1a−c**, which explains why the reaction went on after filtration for these catalysts. The results of TEM and DLS clearly show MOF particles smaller than 200 nm. Besides, the presence of nanoparticles could be shown by the Tyndall effect (Figure 10c). Together with the DLS and AAS data, it is reasonable that nano-MOF particles are responsible for the ongoing reaction. Still, the above centrifugation and filtration experiments cannot fully exclude the possibility of leaching.

Therefore, if only nano-MOFs are indeed responsible for the continued conversion after filtration, it should be possible to separate the nano-MOF particles using an ultracentrifuge with a higher speed of rotation. Reaction of **2-NO_2-d** with methanol and benzaldehyde was run for 1 min to 12% conversion. Then the solution was carefully filtered with a syringe filter as before and additionally centrifuged at 24 000 rpm for 5 min. This procedure lasted 19 min, during which solid **2-NO_2-d** was still in contact with the reaction mixture so that the catalytic reaction could continue. Separation was complete after a total of 20 min. After this 20 min the conversion was monitored on the clear solution in a new vial by GC (Figure 11a). The reaction between MeOH and benzaldehyde came to a stop after removal of solid **2-NO_2-d** through ultracentrifugation. Therefore, we can rule out any leaching of soluble Cr(III) species. This result is supported by DLS measurements of the filtrate after ultracentrifugation, where no particles could be detected anymore.

In order to assess the activity of the **2-NO_2-d** nano-MOF particles, the following experiment was carried out: first, methanol (6.7 mL) was added to **2-NO_2-d** (10 mg), and the resulting suspension was stirred for 10 min. Then the suspension was filtered with the 0.2 μm syringe filter, and benzaldehyde (3.3 mmol) was added to the clear filtrate solution. The catalytic reaction was monitored as before under standard conditions. DLS measurements showed the nano-MOF particles in solution (Figure S14, Supporting Information). The amount of nano-MOF was determined from the filtrate after filtration with the 0.2 μm syringe filter. This filtrate was centrifugated at 24 000 rpm, and the residual solid was weighed to much less than 1 mg. The activity of **2-NO_2-d** after separation of the larger particles (cf. Figure 9) can be compared with the activity of the **2-NO_2-d** nanoparticles alone (Figure 11b). After separation of the larger particles conversion with the remaining nano-MOF particles increased from 63% to 93% over the next 80 min. The amount of less than 1 mg of **2-NO_2-d** nano-MOF alone enables a conversion of 68% in 90 min (Figure 11b). Thus, the small amount of nano-MOFs is much more active than the larger MIL particles.

In conclusion, a much lower sample amount of **2-NO_2-d** (less than 1 mg) can catalyze the acetalization reaction to about 60% conversion after 90 min (Figure 11b), which is nearly the same conversion as achieved for 10 mg of **1a**. This observation can be transferred to the small particle size in **3-NH_2-ps**, which leads to a slightly increased activity despite the lower Brønsted acidity compared to **1a** (Tables 2 and 3).

Recycling/Multiple Run Experiments. The possibility of catalyst recycling was tested for **1a** and **2-NO_2-d** over 5 runs. Catalyst runs were carried out for 90 min each for **1a** and **2-NO_2-d**. For less active **1a** the runs were also extended over 15 h each to achieve nearly quantitative conversion. After the first and fifth runs a PXRD spectrum was recorded to check for catalyst stability (Figure 12).

Catalysts **1a** and **2-NO_2-d** have a relatively stable catalytic activity over 5 runs of 15 h and 90 min, respectivly (Figure 12a). For **1a** the catalytic conversion drops from 73% to 50% for the 90 min runs. After the runs the materials were analyzed for their porosity and crystallinity. The results of the BET surface areas after five runs (90 min each) are for **1a** 3100 m^2/g and for **2-NO_2-d** 2421 m^2/g, (Table 1, Figure S2, Supporting Information), so that the materials retain their initial porosity.

dx.doi.org/10.1021/ic5006456 | Inorg. Chem. 2014, 53, 7319−7333

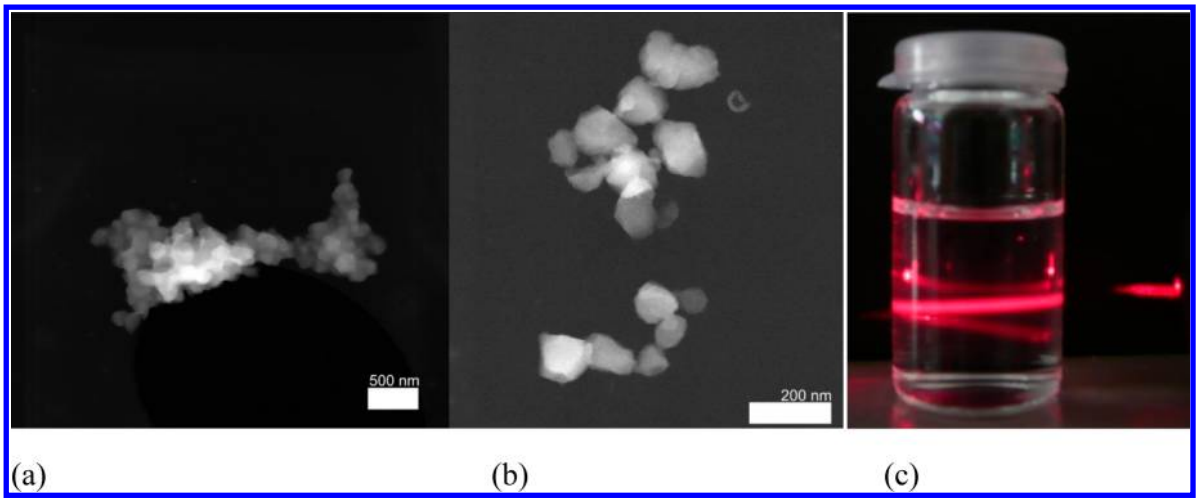

Figure 10. TEM image of the filtrate of **2-NO_2-d** filtered with a 0.2 μm (200 nm) syringe filter after (a) 5 and (b) 10 min. (c) Filtered solution of **2-NO_2-d** showing the Tyndall effect upon 650 nm laser irradiation.

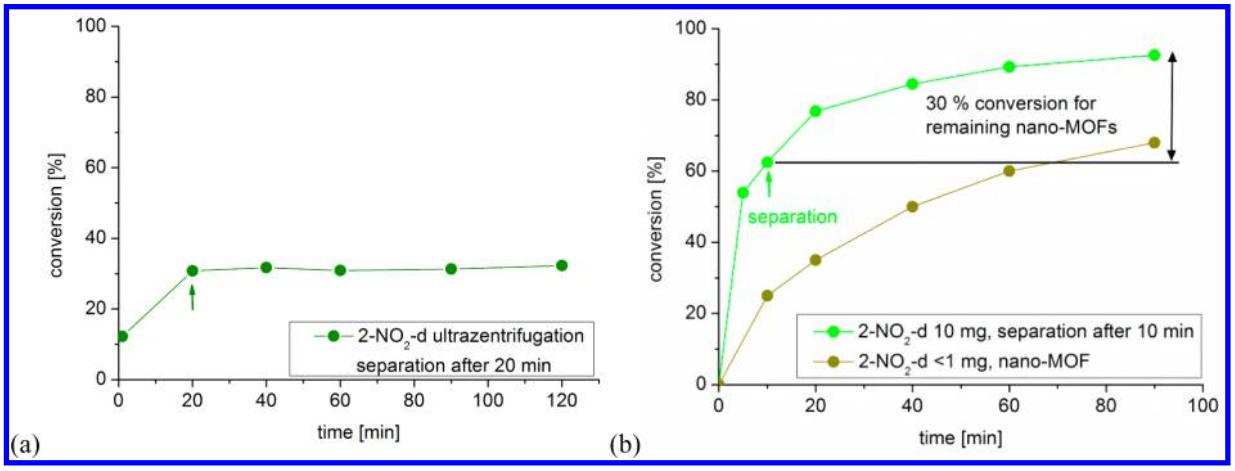

Figure 11. Time conversion plot for (a) **2-NO_2-d** after separation (0.2 μm filtration and 24 000 rpm centrifugation) completed after 20 min and (b) **2-NO_2-d** with attempted separation (6000 rpm centrifugation plus 0.2 μm filtration) of the catalyst completed after 5 min (cf. Figure 9a) and **2-NO_2-d** nano-MOF.

At the same time, the PXRD analysis shows some deterioration of the microcrystallinity and possibly a phase change for **1a** after the five 15 h runs and substantial crystal deterioration and phase change for **2-NO_2-d** after the five 90 min runs (Figure 12b). Yet, **1a** still retains its structure after the five 90 min runs; hence, the nonfunctionalized MOF **1a** is more stable than **2-NO_2-d** under the catalytic conditions. SEM pictures after 5 runs for **1a** and **2-NO_2-d** did not show any significant changes (Figure S15, Supporting Information).

Acetalization Reactivity of 2-NO_2-d with Other Alcohols. MOFs are discussed in terms of heterogeneous catalysts which can possess the selectivity properties of homogeneous catalysts.[20,57] The pores of the MOF are viewed as a "reactor", which can exert selectivity, e.g., by size exclusion effects.[41,58,59] If the reaction does indeed take place mainly inside the pores then the reaction rate should be influenced by the size and shape of the reagents. For larger substrates the diffusion of reagents and products through the pores and pore windows of the MOF material is expected to be slower, and in consequence, the catalyst activity should decrease. MIL-101Cr has pore sizes of 2.9 and 3.4 nm, which are accessible through cage windows of 1.2−1.6 nm (Figure S1, Supporting Information).[22] In order to investigate the effect of the size of the alcohol, the conversion rate with **2-NO_2-d** in the benzaldehyde acetalization reaction is compared in Figure 13a for methanol, ethanol, 1-propanol, 1-butanol, and 1-pentanol.

A decrease of conversion rate with increasing chain length of the homologous *n*-alcohol series can be observed. These results support our expectation and are in agreement with the studies of García and co-workers, who investigated the catalytic activity of $Cu_3(BTC)_2$ in the acetalization of benzaldehyde. Hence, the decrease of conversion rate with increasing alcohol chain length can be ascribed mostly to steric hindrances for substrate diffusion in the pore system.[41] Taking into account that the cage windows of MIL-101Cr with 1.2 and 1.6 nm are bigger compared than the ones of $Cu_2(BTC)_3$ (0.8 nm),[41] this is another important factor for the higher catalyst activity of MIL-101Cr.

Still, even under homogeneous conditions in the absence of steric hindrance on the catalyst center, a longer chain alcohol would be expected to react more slowly. Therefore, the benzaldehyde acetalization reactions were run under homogeneous but otherwise identical conditions with $Cr(NO_3)_3{\cdot}9H_2O$ as catalyst, with the equivalent molar amount of chromium to 10 mg of MIL-101Cr (Figure 13b). After 90 min conversion for all alcohols except pentanol is higher than 82%. A slight

dx.doi.org/10.1021/ic5006456 | Inorg. Chem. 2014, 53, 7319−7333

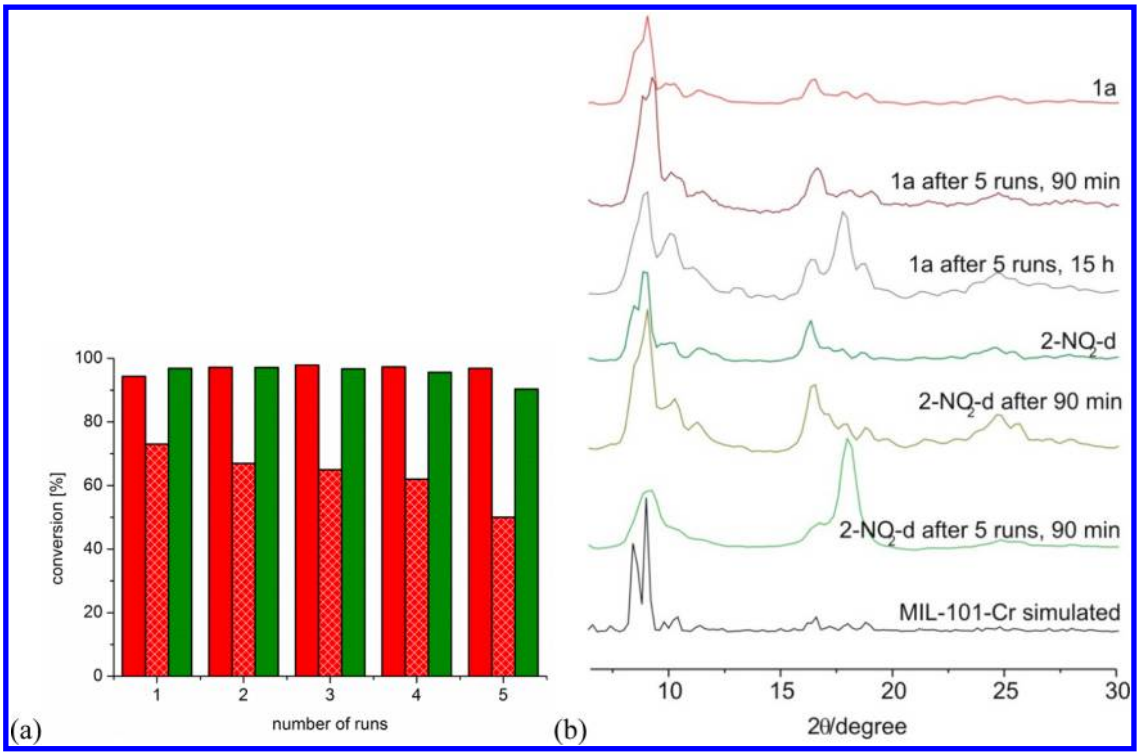

Figure 12. (a) Conversions in catalyst recycling experiments for **1a** (red, each run 15 h; red squared, each run 90 min) and **2-NO_2-d** (green bars). (b) XRD spectra of **1a** and **2-NO_2-d** before and after the catalytic runs.

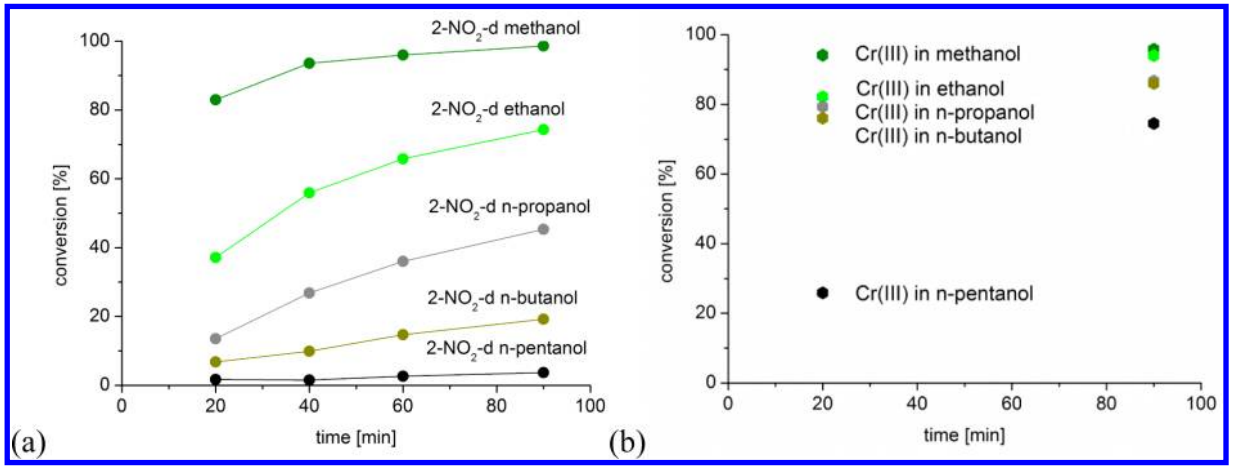

Figure 13. (a) Catalysis of **2-NO_2-d** or (b) chromium(III) nitrate nonahydrate with benzaldehyde in methanol, ethanol, *n*-propanol, *n*-butanol, and *n*-pentanol.

decrease of conversion is seen with increasing alcohol chain length. Yet, even *n*-pentanol gives 75% conversion after 90 min with $Cr(NO_3)_3{\cdot}9H_2O$, compared to only 4% with **2-NO_2-d** (Table S2, Supporting Information). The strong decrease of conversion rate with increasing chain length of the alcohol for **2-NO_2-d** supports the assumption that catalysis occurs mainly inside the pores of the MIL material.

Similarly, different aldehydes were tested under the same standard conditions with **2-NO_2-d** and $Cr(NO_3)_3{\cdot}9H_2O$ as catalyst (Figure 14, Table 5). All benzaldehyde derivatives and cyclohexanone show high and rapid conversion under heterogeneous and homogeneous conditions. Under heterogeneous conditions *p*-chlorobenzaldehyde reacts slower but also reaches over 90% conversion after 90 min. For cyclohexanone the conversion is fast and reaches the final value already after 20 min, where it remains unchanged to 90 min under both hetero- and homogeneous conditions. Noteworthy, conversion of cyclohexanone is higher with **2-NO_2-d** (90%) than with $Cr(NO_3)_3{\cdot}9H_2O$ (84%) as catalyst (Figure 14). Significant is the very low conversion for cyclohexylmethylketone, which is faster with the MIL than in homogeneous solution (Figure 14). The +I effect of the ketone leads to a reduced rate for the attack on the carboxyl carbon atom. It is reported that also for acetophenone and benzophenone no acetalization occurs.[32] Perhaps the higher and faster conversion of the aliphatic ketones cyclohexanone and cyclohexylmethylketone with **2-NO_2-d** compared to $Cr(NO_3)_3{\cdot}9H_2O$ are evidence for a water binding effect of the MIL network.

dx.doi.org/10.1021/ic5006456 | *Inorg. Chem.* 2014, 53, 7319−7333

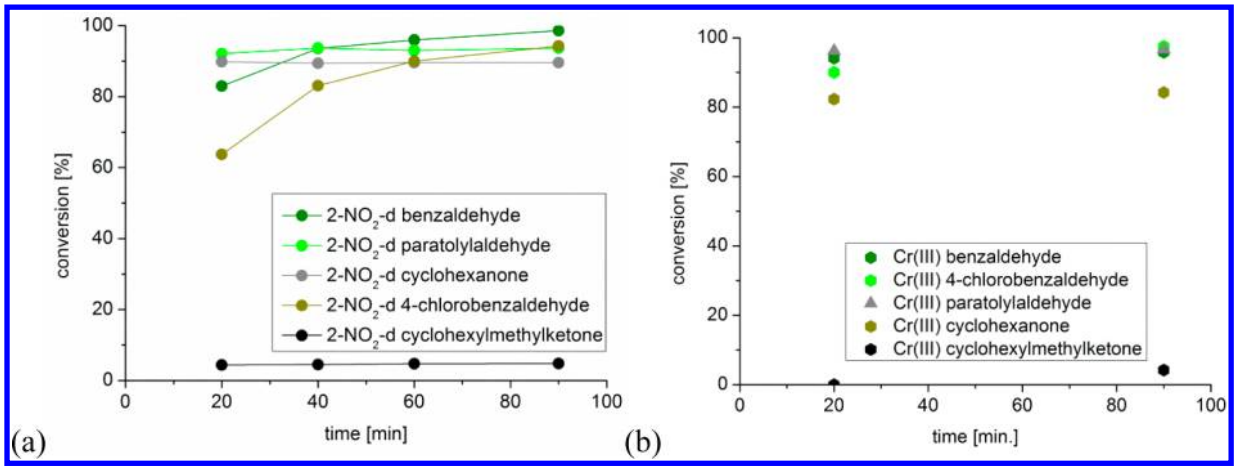

Figure 14. (a) Catalysis of **2-NO_2-d** or (b) chromium(III) nitrate nonahydrate with methanol and different aldehydes or ketones.

Table 5. Reaction of Different Aldehydes and Ketones in Methanol with 2-NO_2-d as Catalyst[a]

Entry	Reagent	Product	Time (min)	Conversion (%)	TON	TOF [h^{-1}]	Conversion (%) [b]
1	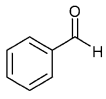	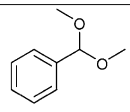	90	99	114	76	96
2	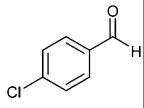	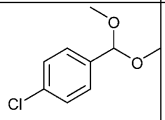	90	94	108	72	98
3	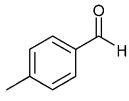	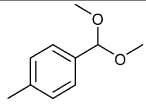	90	94	108	72	97
4	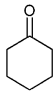	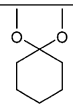	90	90	83	55	84
5	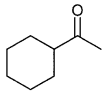	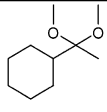	90	5	6	4	4

[a]Standard reaction conditions: aldehyde (3.3 mmol), methanol (166 mmol), catalyst (10 mg); every reaction was performed at least in a duplicate. [b]Conversion after 90 min is stated; 4.2×10^{-5} mol $Cr(NO_3)_3 \cdot 9H_2O$ was used under otherwise identical conditions.

In comparison with other catalysts, the material **2-NO_2-d** displays excellent activity, surpasses other MOFs, and can compete with the homogeneous catalyst $TiCl_4$ (Table 6).

Compared with the results for $Cu_3(BTC)_2$[41] and MIL-100Fe, MIL-101Cr-NO_2 (**2-NO_2-d**) shows a significantly higher catalytic activity for acetalization of benzaldehyde as well as for other aldehydes and alcohols (not shown in Table 6). In particular, for reaction of *p*-tolylaldehyde with methanol **2-NO_2-d** shows 94% conversion after 90 min, which is a significant improvement compared to $Cu_3(BTC)_2$ (ca. 30% after 24 h). These results could be obtained in a shorter time with a much lower catalyst loading and a higher amount of aldehyde (3.3 vs 1 mmol).

CONCLUSIONS

In the diacetalization of aldehydes and ketones with alcohols the high surface area of MIL-101Cr materials is not the decisive factor for high catalytic activity. Introduction of a nitro, $-NO_2$, group to the terephthalate ligand of MIL-101-Cr enhanced the catalytic activity significantly, although the BET surface area of the nitro modification **2-NO_2-d** is lower than that of the nonfunctionalized materials, e.g., **1a**. Compound **2-NO_2-d** is an efficient and a reusable heterogeneous solid catalyst for formation of dimethyl acetals. A possible stronger Lewis acidity through nitro modification is not the primary reason for the excellent activity of **2-NO_2-d**. Instead, pH measurements show that the activity can be explained by Brønsted-acid catalysis from deprotonation of the polarized aqua ligands, which is

dx.doi.org/10.1021/ic5006456 | Inorg. Chem. 2014, 53, 7319−7333

Table 6. Comparison of Different Catalysts for Acetalization of Benzaldehyde in Methanol (B−M reaction)

catalyst	amount of catalyst (mg/mmol metal)[a]	molar ratio benzaldehyde:methanol	temperature (°C)	time (h)	conversion (%)	TOF (h^{-1})[b]	ref
MIL-101/PTA_{imp}	10/0.001 PTA + 0.043 mmol Cr(III)	3.3:166	25	24	93	2.9	29
PTA (phospho-tungstic acid)	0.003[c]	3.3:166	25	24	93	43	29
$Cu_3(BTC)_2$ (HKUST-1, Basolite C300)	50/0.25	1:74	rt	2; 24	63; 88	1.2; 0.2	41
Fe(BTC) (Basolite F300)	50/0.19	1:74	rt	2; 24	49; 71	1.3; 0.2	41
$Al_2(BDC)_3$ (MIL-53Al, Basolite A100)	50/0.24	1:74	rt	24	66	0.12	41
MIL-100Fe	10/0.046	3.0:123	40	5; 21	79:84	10.3; 2.6	57
MIL-101Cr-NO_2, **2-NO_2-d**	10/0.043	3.3:166	rt	1.5	99	50.7	this work
MIL-101Cr-NO_2, **2-NO_2-d**	10/0.043	3.3:166	rt	0.7	94	103	this work
MIL-101-NO_2, **2-NO_2-d** nano-MOF	1/0.0043	3.3:166	rt	1.5	68	348	this work
$TiCl_4/NH_3$	1 mol %/ 0.05 mmol	5.0:246	0	0.5	98	196	33

[a]The milligram amount refers to the total mass of catalyst used; the $mmol_{metal}$ amount refers to the total molar amount of metal in the catalyst mass. No corrections for coordinative unsaturated sites were made. [b]TOF = $mol_{product}/(mol_{metal}\cdot time)$. [c]Total amount PTA in solution (6.7 mL methanol)

strongly enhanced for **2-NO_2-d**. In addition it could be shown that very small amounts of nanoscale MIL particles of **2-NO_2-d** (<200 nm) result already in a high conversion compared with the bulk material. The effect of particle size then increases the activity of the amino modification **3-NH_2-ps** over the nonfunctionalized material **1a** despite a slightly lower Brønsted acidity of the former. By comparing a series of longer chained alcohols with homogeneous $Cr(NO_3)_3$ catalyst it could be shown that catalysis takes place inside the pores of the MIL materials. Therefore, MIL-101Cr and possibly other MILs can be active heterogeneous Brønsted-acid catalysts whose activity can be enhanced by electron-withdrawing linker modifications and small particle size.

■ ASSOCIATED CONTENT

Supporting Information

Synthesis and catalytic procedure details, N_2 sorption isotherms, powder X-ray diffractograms, IR spectra, additional catalytic data, DLS measurements, SEM images, thermogravimetic analysis. This material is available free of charge via the Internet at http://pubs.acs.org.

■ AUTHOR INFORMATION

Corresponding Author

*E-mail: janiak@uni-duesseldorf.de.

Notes

The authors declare no competing financial interest.

■ ACKNOWLEDGMENTS

Our work was supported by the Deutsche Forschungsgemeinschaft (DFG grant Ja466/25-1) and the University of Düsseldorf. We thank Mr. Hajo Meyer for providing the TEM images.

■ DEDICATION

Dedicated to Prof. Christel Marian on the occasion of her 60th birthday.

■ REFERENCES

(1) (a) Collins, D. J.; Zhou, H.-C. *J. Mater. Chem.* **2007**, *17*, 3154−3160. (b) Dincă, M.; Long, J. R. *Angew. Chem., Int. Ed.* **2008**, *47*, 6766−6779. (c) Lin, X.; Jia, J.; Hubberstey, P.; Schröder, M.; Champness, N. R. *CrystEngComm* **2007**, *9*, 438−448. (d) Ma, S.; Zhou, H.-C. *Chem. Commun.* **2010**, *46*, 44−53. (e) Morris, R. E.; Wheatley, P. S. *Angew. Chem., Int. Ed.* **2008**, *47*, 4966−4981. (f) Murray, L. J.; Dincă, M.; Long, J. R. *Chem. Soc. Rev.* **2009**, *38*, 1294−1314. (g) Suh, M. P.; Park, H. J.; Prasad, T. K.; Lim, D.-W. *Chem. Rev.* **2012**, *112*, 782−835. (h) Getman, R. B.; Bae, Y.-S.; Wilmer, C. E.; Snurr, R. Q. *Chem. Rev.* **2012**, *112*, 703−723.

(2) (a) Tanh Jeazet, H. B.; Staudt, C.; Janiak, C. *Dalton Trans.* **2012**, *41*, 14003−14027. (b) Hunger, K.; Schmeling, N.; Tanh Jeazet, H. B.; Janiak, C.; Staudt, C.; Kleinermanns, K. *Membranes* **2012**, *2*, 727−763. (c) Tanh Jeazet, H. B.; Staudt, C.; Janiak, C. *Chem. Commun.* **2012**, *48*, 2140−2142. (d) Li, J.-R.; Sculley, J.; Zhou, H.-C. *Chem. Rev.* **2012**, *112*, 869−932. (e) Zhang, Z.; Zhao, Y.; Gong, Q.; Li, Z.; Li, J. *Chem. Commun.* **2013**, *49*, 653−661. (f) Férey, G.; Serre, C.; Devic, T.; Maurin, G.; Jobic, H.; Llewellyn, P. L.; De Weireld, G.; Vimont, A.; Daturi, M.; Chang, J. S. *Chem. Soc. Rev.* **2011**, *40*, 550−562. (g) Zornoza, B.; Tellez, C.; Coronas, J.; Gascon, J.; Kapteijn, F. *Microporous Mesoporous Mater.* **2013**, *166*, 67−78. (h) Dong, G. X.; Li, H. Y.; Chen, V. K. *J. Mater. Chem. A* **2013**, *1*, 4610−4630.

(3) (a) Kreno, L. E.; Leong, K.; Farha, O. K.; Allendorf, M.; Van Duyne, R. P.; Hupp, J. T. *Chem. Rev.* **2012**, *112*, 1105−1125. (b) Janiak, C.; Vieth, J. K. *New J. Chem.* **2010**, *34*, 2366−2388.

(4) (a) Horcajada, P.; Chalati, T.; Serre, C.; Gillet, B.; Sebrie, C.; Baati, T.; Eubank, J. F.; Heurtaux, D.; Clayette, P.; Kreuz, C.; Chang, J.-S.; Hwang, Y. K.; Marsaud, V.; Bories, P.−N.; Cynober, L.; Gil, S.; Férey, G.; Couvreur, P.; Gref, R. *Nat. Mater.* **2010**, *9*, 172−178. (b) Horcajada, P.; Gref, R.; Baati, T.; Allan, P. K.; Maurin, G.; Couvreur, P.; Férey, G.; Morris, R. E.; Serre, C. *Chem. Rev.* **2012**, *112*, 1232−1268. (c) Keskin, S.; Kızılel, S. *Ind. Eng. Chem. Res.* **2011**, *50*, 1799−1812.

(5) (a) Allendorf, M. D.; Bauer, C. A.; Bhakta, R. K.; Houk, R. J. T. *Chem. Soc. Rev.* **2009**, *38*, 1330−1352. (b) Cui, Y.; Yue, Y.; Qian, G.; Chen, B. *Chem. Rev.* **2012**, *112*, 1126−1162.

(6) (a) Kepert, C. J. *Chem. Commun.* **2006**, *21*, 695−700. (b) Kurmoo, M. *Chem. Soc. Rev.* **2009**, *38*, 1353−1379. (c) Maspoch, D.; Ruiz-Molina, D.; Veciana, J. *J. Mater. Chem.* **2004**, *14*, 2713−2723.

(7) (a) Farrusseng, D.; Aguado, S.; Pinel, C. *Angew. Chem., Int. Ed.* **2009**, *48*, 7502−7513. (b) Lee, J. Y.; Farha, O. K.; Roberts, J.; Scheidt, K. A.; Nguyen, S. T.; Hupp, J. T. *Chem. Soc. Rev.* **2009**, *38*, 1450−1459. (c) Ranocchiari, M.; van Bokhoven, J. A. *Phys. Chem. Chem. Phys.* **2011**, *13*, 6388−6396. (d) Dhakshinamoorthy, A.; Alvaro, M.; Garcia, H. *Chem. Commun.* **2012**, *48*, 11275−11288. (e) Dhakshinamoorthy, A.; Opanasenko, M.; Čejka, J.; Garcia, H. *Adv. Synth. Catal.* **2013**, *355*, 247−268.

dx.doi.org/10.1021/ic5006456 | *Inorg. Chem.* 2014, 53, 7319−7333

(8) (a) Henninger, S. K.; Jeremias, F.; Kummer, H.; Janiak, C. *Eur. J. Inorg. Chem.* **2012**, 2625−2634. (b) Akiyama, G.; Matsuda, R.; Sato, H.; Hori, A.; Takata, M.; Kitagawa, S. *Microporous Mesoporous Mater.* **2012**, *157*, 89−93. (c) Akiyama, G.; Matsuda, R.; Kitagawa, S. *Chem. Lett.* **2010**, *39*, 360−361. (d) Jeremias, F.; Khutia, A.; Henninger, S. K.; Janiak, C. *J. Mater. Chem.* **2012**, *22*, 10148−10151. (e) Küsgens, P.; Rose, M.; Senkovska, I.; Fröde, H.; Henschel, A.; Siegle, S.; Kaskel, S. *Microporous Mesoporous Mater.* **2009**, *120*, 325−330. (f) Ehrenmann, J.; Henninger, S. K.; Janiak, C. *Eur. J. Inorg. Chem.* **2011**, 471−474. (g) Seo, Y.-K.; Yoon, J. W.; Lee, J. S.; Hwang, Y. K.; Jun, C.-H.; Chang, J.-S.; Wuttke, S.; Bazin, P.; Vimont, A.; Daturi, M.; Bourrelly, S.; Llewellyn, P. L.; Horcajada, P.; Serre, C.; Férey, G. *Adv. Mater.* **2012**, *24*, 806−810. (h) Henninger, S. K.; Habib, H. A.; Janiak, C. *J. Am. Chem. Soc.* **2009**, *131*, 2776−2777. (i) Khutia, A.; Urs Rammelberg, H.; Schmidt, T.; Henninger, S.; Janiak, C. *Chem. Mater.* **2013**, *25*, 790−798. (j) Jeremias, F.; Lozan, V.; Henninger, S.; Janiak, C. *Dalton Trans.* **2013**, *42*, 15967−15973.

(9) (a) Moon, H. R.; Kim, J. H.; Paik Suh, M. *Angew. Chem., Int. Ed.* **2005**, *44*, 1261−1265. (b) Hermes, S.; Schröder, M.-K.; Schmid, R.; Knodeir, L.; Muhler, M.; Tissler, A.; Fischer, R. W.; Fischer, R. A. *Angew. Chem., Int. Ed.* **2005**, *44*, 6237−62411261. (c) Sabo, M.; Henschel, A.; Froede, H.; Klemm, E.; Kaskel, S. *J. Mater. Chem.* **2007**, *17*, 3827−3832. (d) Müller, M.; Hermes, S.; Kähler, K.; Van den Berg, M. W. E.; Muhler, M.; Fischer, R. A. *Chem. Mater.* **2008**, *20*, 4576−4587. (e) Dhakshinamoorthy, A.; Garcia, H. *Chem. Soc. Rev.* **2012**, *41*, 5262−5284.

(10) Stock, N.; Biswas, S. *Chem. Rev.* **2012**, *112*, 933−969.

(11) (a) Lee, J. Y.; Farha, O. K.; Roberts, J.; Scheidt, K. A.; Nguyena, S. T.; Hupp, J. T. *Chem. Soc. Rev.* **2009**, *38*, 1450−1459. (b) Phan, N. T. S.; Nguyen, T. T.; Ho, P.; Nguyen, K. D. *ChemCatChem* **2013**, *5*, 1822−1831. (c) Huang, Y.; Liu, T.; Lin, J.; Lü, J.; Lin, Z.; Cao, R. *Inorg. Chem.* **2011**, *50*, 2191−2198. (d) Horike, S.; Dincă, M.; Tamaki, K.; Long, J. R. *J. Am. Chem. Soc.* **2008**, *130*, 5854−5855.

(12) Dhakshinamoorthy, A.; Alvaro, M.; Corma, A.; Garcia, H. *Dalton Trans.* **2011**, *40*, 6344−6360.

(13) (a) Alaerts, L.; Seguin, E.; Poelman, H.; Thibault-Starzyk, F.; Jacobs, P. A.; De Vos, D. E. *Chem.—Eur. J.* **2006**, *12*, 7353−7363. (b) Gándara, F.; Gomez-Lor, B.; Gutiérrez-Puebla, E.; Iglesias, M.; Monge, M. A.; Proserpio, D. M.; Snejko, N. *Chem. Mater.* **2008**, *20*, 72−76.

(14) Schlichte, K.; Kratzke, T.; Kaskel, S. *Microporous Mesoporous Mater.* **2004**, *73*, 81−88.

(15) Valvekens, P.; Vermoortele, F.; De Vos, D. *Catal. Sci. Technol.* **2013**, *3*, 1435−1445.

(16) Van de, Voorde B.; Boulhout, M.; Vermoortele, F.; Horcajada, P.; Cunha, D.; Lee, J. S.; Chang, J.; Gibson, E.; Daturi, M.; Lavalley, J.; Vimont, A.; Beurroies, I.; De Vos, D. E. *J. Am. Chem. Soc.* **2013**, *135*, 9849−9856.

(17) Hwang, Y. K.; Hong, D.-Y.; Chang, J.-S.; Jhung, S. H.; Seo, Y.-K.; Kim, J.; Vimont, A.; Daturi, M.; Serre, C.; Férey, G. *Angew. Chem., Int. Ed.* **2008**, *47*, 4144−4148.

(18) Savonnet, M.; Ravon, U.; Aguado, S.; Bazer-Bachi, D.; Lecocq, V.; Bats, N.; Pinel, C.; Farrusseng, D. *Green Chem.* **2009**, *11*, 1729−1732.

(19) Gascon, J.; Aktay, U.; Hernandez-Alonso, M. D.; van Klink, G. P. M.; Kapteijn, F. *J. Catal.* **2009**, *261*, 75−87.

(20) Vermoortele, F.; Bueken, B.; Le Bars, G.; Van de Voorde, B.; Vandichel, M.; Houthoofd, K.; Vimont, A.; Daturi, M.; Waroquier, M.; Van Speybroeck, V.; Kirschhock, C.; De Vos, D. E. *J. Am. Chem. Soc.* **2013**, *135*, 11465−11468.

(21) Vermoortele, F.; Vandichel, M.; Van de Voorde, B.; Ameloot, R.; Waroquier, M.; Van Speybroeck, V.; De Vos, D. E. *Angew. Chem., Int. Ed.* **2012**, *51*, 4887−4890.

(22) Férey, G.; Mellot-Draznieks, C.; Serre, C.; Millange, F.; Dutour, J.; Surblé, S.; Margiolaki, I. *Science* **2005**, *309*, 2040−2042.

(23) Hong, D.-Y.; Hwang, Y. K.; Serre, C.; Férey, G.; Chang, J.-S. *Adv. Funct. Mater.* **2009**, *19*, 1537−1552.

(24) Hwang, Y. K.; Hong, J.-S.; Chang, D.-Y.; Seo, H.; Yoon, M.; Kim, J.; Jhung, S. H.; Serre, C.; Férey, G. *Appl. Catal. A: Gen.* **2009**, *358*, 249−253.

(25) (a) Granadeiro, C. M.; Barbosa, A. D. S.; Silva, P.; Almeida Paz, F. A.; Saini, V. K.; Pires, J.; de Castro, B.; Balula, S. S.; Cunha-Silva, L. *Appl. Catal. A: General* **2013**, *453*, 316−326. (b) Maksimchuk, N. V.; Kovalenko, K. A.; Arzumanov, S. S.; Chesalov, Y. A.; Melgunov, M. S.; Stepanov, A. G.; Fedin, V. P.; Kholdeeva, O. A. *Inorg. Chem.* **2010**, *49*, 2920−2930.

(26) Henschel, A.; Gedrich, K.; Kraehnert, R.; Kaskel, S. *Chem. Commun.* **2008**, 4192−4194.

(27) Hartmann, M.; Fischer, M. *Microporous Mesoporous Mater.* **2012**, *164*, 38−43.

(28) Wu, F.; Qiu, L.-G.; Ke, F.; Jiang, X. *Inorg. Chem. Commun.* **2013**, *32*, 5−8.

(29) Bromberg, L.; Hatton, T. A. *ACS Appl. Mater. Interfaces* **2011**, *3*, 4756−4764.

(30) Brückner, R. *Advanced Organic Chemistry: Reaction Mechanisms*; Harcourt/Academic Press: Burlington, MA, 2002; p 291.

(31) Miao, J.; Wan, H.; Shao, Y.; Guan, G.; Xu, B. *J. Mol. Catal. A: Chem.* **2011**, *348*, 77−82.

(32) Krompiec, S.; Penkala, M.; Szczubiałka, K.; Kowalska, E. *Coord. Chem. Rev.* **2012**, *256*, 2057−2095.

(33) Clerici, A.; Pastori, N.; Porta, O. *Tetrahedron* **1998**, *54*, 15679−15690.

(34) Jiang, Q.; Rüegger, H.; Venanzi, L. M. *Inorg. Chim. Acta* **1999**, *290*, 64−79.

(35) Vermoortele, F.; Ameloot, R.; Vimont, A.; Serre, C.; De Vos, D. *Chem. Commun.* **2011**, *47*, 1521−1523.

(36) Xu, F.-C.; Krouse, H. R.; Swaddle, T. W. *Inorg. Chem.* **1985**, *24*, 267−270.

(37) Corma, A.; Climent, M. J.; García, H.; Primo, J. *J. Appl. Catal.* **1990**, *59*, 333−340.

(38) Kamitori, Y.; Hojo, M.; Masuda, R.; Yoshida, T. *Tetrahedron Lett.* **1985**, *26*, 4767−4770.

(39) Climent, M. J.; Corma, A.; Iborra, S.; Navarro, M. C.; Primo, J. *J. Catal.* **1996**, *161*, 783−789.

(40) Tanaka, Y.; Sawamura, N.; Iwamoto, M. *Tetrahedron Lett.* **1998**, *39*, 9457−9460.

(41) Dhakshinamoorthy, A.; Alvaro, M.; García, H. *Adv. Synth. Catal.* **2010**, *352*, 3022−3030.

(42) Srirambalaji, R.; Hong, S.; Natarajan, R.; Yoon, M.; Hota, R.; Kim, Y.; Ko, Y. H.; Kim, K. *Chem. Commun.* **2012**, *48*, 11650−11652.

(43) Vimont, A.; Leclerc, H.; Mauge, F.; Daturi, M.; Lavalley, J.; Surble, S.; Serre, C.; Férey, G. *J. Phys. Chem. C* **2007**, *111*, 383−388.

(44) Volkringer, C.; Leclerc, H.; Lavalley, J.; Loiseau, T.; Férey, G.; Daturi, M.; Vimont, A. *J. Phys. Chem. C* **2012**, *116*, 5710−5719.

(45) Yang, J.; Zhao, Q.; Li, J.; Dong, J. *Microporous Mesoporous Mater.* **2010**, *130*, 174−179.

(46) Bernt, S.; Guillerm, V.; Serre, C.; Stock, N. *Chem. Commun.* **2011**, *47*, 2838−2840.

(47) Modrow, A.; Zargarani, D.; Herges, R.; Stock, N. *Dalton Trans.* **2012**, *41*, 8690−8696.

(48) (a) Cohen, S. M. *Chem. Rev.* **2012**, *112*, 970−1000. (b) Valtchev, V.; Majano, G.; Mintova, S.; Pérez-Ramírez, J. *Chem. Soc. Rev.* **2013**, *42*, 263−290.

(49) Emerson, K.; Graven, W. M. *J. Inorg. Nucl. Chem.* **1959**, *11*, 309−313.

(50) Hughes, R. G.; Garner, C. S. *Inorg. Chem.* **1968**, *7*, 1988−1993.

(51) Williams, T. J.; Garner, C. S. *Inorg. Chem.* **1969**, *8*, 1639−1645.

(52) Basolo, F.; Pearson, R. G. *Mechanisms of Inorganic Reactions*, 2nd ed.; John Wiley & Sons, Inc.: New York,1967; p 32.

(53) Andersen, P.; Døssing, A.; Glerup, J.; Rude, M. *Acta Chem. Scand.* **1990**, *44*, 346−352.

(54) Ashley, K. R.; Kulphrathipanja, S. *Inorg. Chem.* **1972**, *11*, 444−447.

(55) Vermoortele, F.; Ameloot, R.; Alaerts, L.; Matthessen, R.; Carlier, B.; Fernandez, E. V. R.; Gascon, J.; Kapteijn, F.; De Vos, D. E. *J. Mater. Chem.* **2012**, *22*, 10313−10321.

(56) Capeletti, M. R.; Balzano, L.; de la Puente, G.; Laborde, M.; Sedran, U. *Appl. Catal., A* **2000**, L1−L4.
(57) Dhakshinamoorthy, A.; Alvaro, M.; Horcajada, P.; Gibson, E.; Vishnuvarthan, M.; Vimont, A.; Greneche, J.; Serre, C.; Daturi, M.; García, H. *ACS Catal.* **2012**, *2*, 2060−2065.
(58) Luo, Q.; Ji, M.; Lu, M.; Hao, C.; Qiu, J.; Li, Y. *J. Mater. Chem. A* **2013**, *1*, 6530−6534.
(59) Hermannsdörfer, J.; Friedrich, M.; Kempe, R. *Chem.—Eur. J.* **2013**, *19*, 13652−13657.

dx.doi.org/10.1021/ic5006456 | *Inorg. Chem.* 2014, 53, 7319−7333